Is *d*–AlCuCo a Random Tiling?

Gabriele Zeger[1,a], Dieter Plachke[a,b], Heinz Dieter Carstanjen[a,b], and Hans-Rainer Trebin[a]

[a] *Institut für Theoretische und Angewandte Physik, Universität Stuttgart, Pfaffenwaldring 57, D-70550 Stuttgart, Germany*
[b] *Max–Planck–Institut für Metallforschung, Heisenbergstr.1, D-70569 Stuttgart, Germany*

Received

Abstract

Channeling Monte Carlo simulations, in combination both with Rutherford backscattering (RBS) and particle-induced x-ray emission (PIXE), have been performed on model quasicrystals of decagonal AlCuCo with different amount of phason disorder. Comparing our simulation results to experimental data we obtain the best agreement for those models with a large amount of phason disorder. This leads us to the conclusion that the sample of d-AlCuCo used in the measurements is a random tiling. Beside the aspect of phason disorder we also examined the Cu and Co distribution given by the Burkov models (S.E. Burkov, Phys. Rev. B 47 (1993) 12325). We show that the chemical distribution is in contrast to the experimental PIXE yield profiles. By exchanging some of the Cu and Co positions it is possible to eliminate the discrepancy.

Keywords: Quasicrystals, Random Tilings, Channeling

1. Introduction

More than 15 years after the discovery of quasicrystals structure modeling is still an active field. One interesting aspect is the phason degree of freedom and the question whether quasicrystals are random tilings or deterministically ordered. In a tiling description phason motion becomes evident through simpleton flips of vertices. Many groups have investigated the consequences of phasons. Katz and Kalugin suggested that phason flips induce a new mode of self-diffusion [1]. Recent measurements of the diffusion constant in *i*–AlMnPd by Blüher *et al.* indeed indicate that low-temperature diffusion occurs via a phason assisted mechanism [2]. In this paper we will focus on another feature of phason disorder, namely, how it influences channeling Rutherford backscattering (RBS) and particle induced x–ray emission (PIXE) profiles in decagonal AlCuCo. With the same tools we study the chemical distribution of Cu and Co.

2. Description of the model and channeling

AlCuCo has been one of the first T phases to be grown from the melt up to *mm*-sized thermodynamically stable single crystals, so that in many places detailed structure analysis has been performed on this phase and its isostructural partner *d*-AlNiCo [3, 4, 5]. Most decisive has been a Patterson analysis by Steurer [6]. Several binary model quasicrystals were derived according to which AlCuCo and AlNiCo consist of two plane decagonal quasicrystalline layers, alternatively stacked along a perpendicular tenfold screw axis with a stacking period of 4.18 Å. Among these models are those of Burkov for AlCuCo [7, 8]. A new feature of the most recent two Burkov models [8] is the use of the matching rules of the Tübingen triangle tiling to distinguish between Cu and Co, thus obtaining to our knowledge the first ternary models of AlCuCo.
A further important aspect is that x-ray investigations of both T phases (AlCuCo and AlNiCo) by Frey and Steurer [9] display an appreciable diffuse background and thus indicate a large amount of disorder. Therefore it is necessary not only to study deterministic models of AlCuCo, but also models with pha-

son disorder. Since we have provided a modification of one of the Burkov models in which it is possible to introduce phasons [10], we will use it for phason disorder in AlCuCo. To test the models which have been derived from x-ray investigations we used an experiment in real space. Carstanjen *et al.* performed fast ion channeling on *d*-AlCuCoSi combined with Rutherford backscattering (RBS) to study the decoration of the T-phase structure [11]. Here Cu and Co on one side and Al and Si on the other could not be distinguished [12, 14]. To investigate the distribution

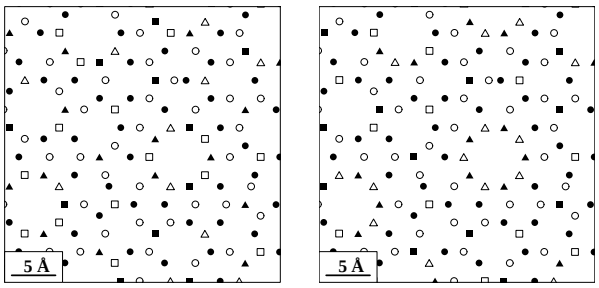

Fig. 1. Left: part of the AlCuCo model BII. Right: part of the AlCuCo model MII. The atomic positions in the two layers are projected along the decagonal axis, layer one with filled and layer two with empty symbols. The symbols are squares for Co, triangles for Cu, and circles for Al.

of chemical species in the Burkov models the characteristic ion–induced K_α-X-ray emission (PIXE) was measured additionally [14]. The yield profiles provide a significant difference for Cu and Co which, as we have shown, cannot be confirmed by the Burkov models [15].

In this paper we will discuss our results on the example of one of the Burkov models (BII) and our modification thereof (MII). The complete description of the PIXE simulations for both Burkov models and our modifications may be found in [15, 16], a detailed discussion of the RBS simulations, not only on the Burkov models, will be presented in a future paper [17]. The composition is calculated to $Al_{62}Cu_{19}Co_{19}$ for the Burkov model (BII) and to $Al_{62}Cu_{24}Co_{14}$ for our modification (MII). In Fig. 1 sections of BII and MII are shown.

The channeling experiments were performed at room temperature; the PIXE data and additionally RBS data for the transition metal (TM) yield were measured with a beam of 3 MeV $^4He^+$-ions and the remaining RBS data were measured with a beam of 2 MeV $^4He^+$-ions [14]. The angular spread was $\pm 0.05^\circ$ due to the experimental beam geometry and the mosaic spread of the sample as determined by x-ray diffraction amounted to 0.07° (FWHM). From these measurements the presence of the microtwinned (5,7) approximant phase can be excluded. Three angular scans were run: an axial one across the decagonal axis and two planar ones inclined by 5° to the decagonal axis: i) along the so called "main planes", and ii) rotatetd by $\Delta\varphi = 18^\circ$ and only in RBS along the "shallower planes" [14]. To compare the models with experimental data, Monte Carlo channeling simulations have been performed. The details of the simulations are published in [16] and references therein.

3. Results and discussion

Since the PIXE simulations have been already described in [15] we will mention the main issues only briefly. The simulation results on BII and MII of the minimum yield $\chi_{\min}$ for ion incidence in a channeling direction and halfwidth values (HWHM) $\Psi_{\frac{1}{2}}$ are documented in Tab.1. Compared to experiment the values for $\chi_{\min}$ are too low both in the axial and planar case; the $\Psi_{\frac{1}{2}}$ values are good in the axial case but much too small in the planar case. In contrast to experiment the Cu and Co profiles of BII are not distinguishable. The simulations for MII produce the correct experimental sequence of $\chi_{\min,\mathrm{Al}}$ as the lowest one, then $\chi_{\min,\mathrm{Co}}$ and finally $\chi_{\min,\mathrm{Cu}}$. A good agreement with experiment is achieved by introducing a certain amount of phason disorder in the MII model (Fig.4 left, [15]).

Fig. 3 shows the RBS yields for the MII model [18] in comparison with experimental data. In the axial case there is a quite good coincidence with the experiment, only the values of $\chi_{\min}$ are a bit smaller. In the case of planar channeling the agreement is getting worse. The RBS Al yield profile of the main planes do not exhibit the pronounced shoulders of the experimental yield profile; also the RBS yield profile of the transition metals (TM) is too deep. The worst discrepancy between experiment and simulation occurs in the case of channeling in the shallower planes. Whereas in the experiment a deep Al yield profile and a flat TM yield profile exist, this is opposite in the simulation. Here the TM yield profile is the deep profile and the Al profile is the flat one. The reason for the too flat Al yield profile, as in other models of AlCuCo, too, is that the Al atoms with the symmetric fivestar as atomic surface contribute with an enhanced backscattering probability along the shallower planes. The Al atoms with the decagons as atomic surfaces, however, contribute to a deep yield profile along the same direction [15, 16]. Thus, the complete Al yield profile shows the flat profile as depicted in Fig. 3 at the right side.

Like in the case of the PIXE profiles the question remains whether the discrepancies described above for the RBS profiles can be explained by phason disorder, as up to now the RBS simulations were perfor-

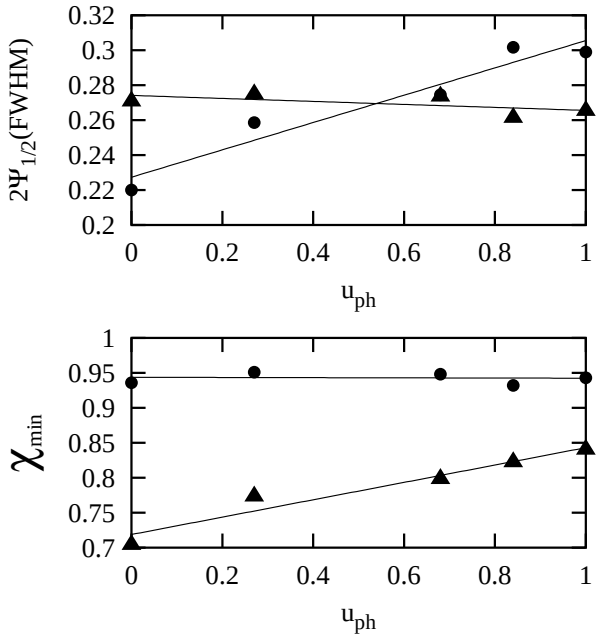

Fig. 2. Simulated $\chi_{\min}$ and $2\Psi_{\frac{1}{2}}$ (FWHM) for different phason disorder for MII in the case of planar channeling with 2 MeV $^4He^+$-ions and an angular spread of $\pm 0.05^\circ$ in the shallower planes, both for the Al (•) and TM (▲) RBS yield profiles. The lines represent a linear least square fit.

med on a perfect model quasicrystal. We constructed four configurations of MII with different amount of phason disorder by introducing phason flips as described in [10, 15]. For the characterization of the phason degree of disorder ($u_{\rm ph}$) we use the normalized deviation of the coordinates in perpendicular space with respect to he ideal quasicrystal [15, 16]. In Fig. 2 the results for planar channeling in the shallower planes was presented. With $u_{\rm ph}$ also the too small $\chi_{\rm min,TM}$ value is increasing whereas the too big $\chi_{\rm min,Al}$ remains nearly constant. Concerning the $\Psi_{\frac{1}{2}}$ values it is reversed; here $\Psi_{\frac{1}{2},\rm Al}$ is increasing with $u_{\rm ph}$, whereas $\Psi_{\frac{1}{2},\rm TM}$ remains nearly constant. The interesting point is that $u_{\rm ph}$ influences the yield profiles of the various atomic species differently unlike most of the other profile changing effects.

All the simulations mentioned above have been performed with an angular spread of $\pm 0.05^\circ$ which is fixed by the beam geometry of the experiment; in reality the angular spread is slightly higher, due to the mosaic spread of the quasicrystal. In Fig. 4 the calculated PIXE and RBS profiles for a MII crystal with $u_{\rm ph} = 0.27$ and an angular spread of $\pm 0.1^\circ$ are directly compared to the measurements for axial channeling along the decagonal axis and planar channeling along the main planes. The agreement is excellent apart from the shoulders of the Al RBS yield profile (Fig.4 bottom right), which is due to extreme sensitivity towards minute deviations of Al positions,

	Al-yield		Cu-yield		Co-yield	
	$\chi_{\rm min}$	$2\Psi_{\frac{1}{2}}$	$\chi_{\rm min}$	$2\Psi_{\frac{1}{2}}$	$\chi_{\rm min}$	$2\Psi_{\frac{1}{2}}$
BII (ax)	0.15	0.55	0.15	0.75	0.15	0.70
MII (ax)	0.15	0.58	0.16	0.80	0.15	0.77
Exp.(ax)	0.42	0.58	0.57	0.78	0.53	0.81
BII (pl)	0.75	0.23	0.84	0.23	0.84	0.23
MII (pl)	0.74	0.25	0.85	0.25	0.81	0.27
Exp.(pl)	0.91	0.37	0.96	0.32	0.94	0.41

Table 1. Axial (above) channeling and planar (below) channeling in the main planes: Simulated $\chi_{\rm min}$ and $2\Psi_{\frac{1}{2}}$ [deg] (FWHM) in the case of PIXE for the two models without phason disorder compared with the experimental data with an angular spread of $\pm 0.05^\circ$. The error of the experimental data is $\pm$ 0.01 for $\chi_{\rm min}$. At $2\Psi_{\frac{1}{2}}$ it is $\pm 0.01^\circ$ for axial channeling and $\pm 0.1^\circ$ for planar channeling [13].

as discussed in [15, 16].

Thus, we conclude that the AlCuCo quasicrystal used in the experiment is described by a random tiling. Other profile changing effects, as vacancies or microcrystalline states, do not change the RBS yield profile such as to explain the discrepancies for planar channeling in the shallower planes [16].

4. Acknowledgements

The authors would like to thank G. Groos and A. Rüdinger for helpful discussion. This work has been supported by the Deutsche Forschungsgemeinschaft under Projects number No. CA 122/3-2 and No. RO 924/4-1.

References

[1] P.A. Kalugin, A. Katz, Europhys. Lett. 21 (1993) 921-925.

[2] R. Blüher *et al.* Phys. Rev. Lett. 80 (1998) 1014-1018.

[3] A.R. Kortan *et al.*, Phys. Rev. Lett. 64 (1990) 200-204.

[4] K. Hiraga, W. Sun, F.J. Lincoln, Jpn. J. Mod. Phys. 30 (1991) L301.

[5] W. Steurer, K.H. Kuo, Philos. Mag. Lett. 62 (1990) 175.

[6] W. Steurer, Acta. Crystallogr. Sect. B 46 (1990) 703.

[7] S.E. Burkov, Phys. Rev. Lett. 67 (1991) 614.

[8] S.E. Burkov, Phys. Rev. B 47 (1993) 12325.

[9] F. Frey, W. Steurer, J. Non-Cryst. Solids 153&154 (1993) 600.

[10] G. Zeger, H.-R. Trebin, Phys. Rev. B 54 (1996) R720.

[11] H.D. Carstanjen *et al.* Phys. Rev. B 45 (1992) 10822.

[12] H.D. Carstanjen, *et al.*, Nucl. Inst. Meth. B 67 (1992) 173.

[13] D. Plachke, PhD thesis, University of Stuttgart (1999).

[14] D. Plachke *et al.*, J. Non-Cryst. Solids 153&154 (1993) 72-76.

[15] G. Zeger *et al.*, Phys. Rev. Lett. 82 (1999) 5273-5277.

[16] G. Zeger, PhD thesis, University of Stuttgart (1999)

[17] G. Zeger, H.-R. Trebin, in preparation

[18] The RBS simulations on the BII model exhibits the same RBS yield profiles as the MII model due to the indistinguishability of the Cu and Co atoms in the RBS experiment.

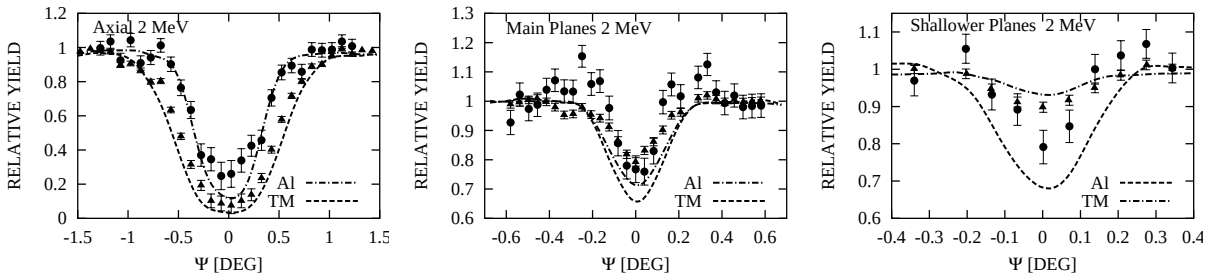

Fig. 3. RBS yield profiles obtained from angular scans across the decagonal axis, the main planar system and the shallower planar system (from left to right). The experimental data is shown with errowbars for T-phase $Al_{62}Cu_{20}Co_{15}Si_3$ with circles for the Al and triangles for the TM atoms. The lines represent the calculated profiles for the MII model with no phason disorder and an angular spread of $\pm 0.05^\circ$.

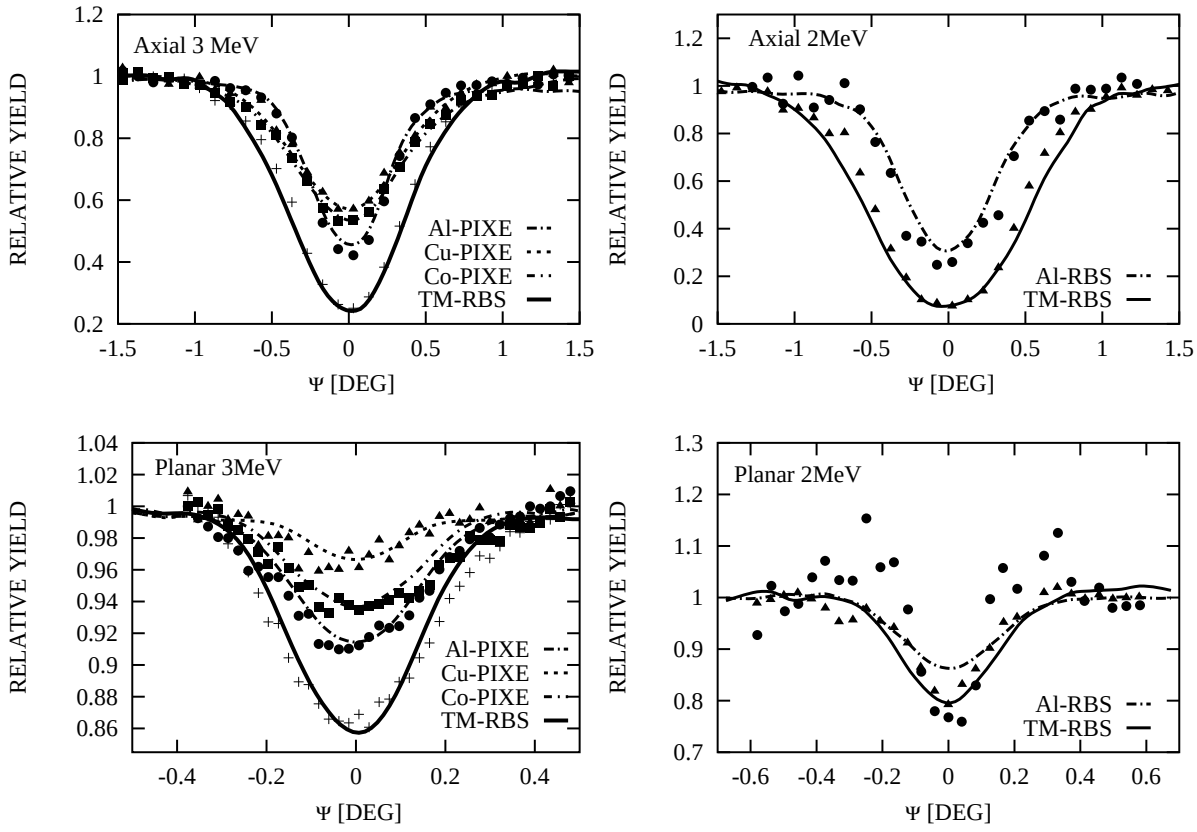

Fig. 4. PIXE and RBS yield profiles as obtained from angular scans across the decagonal axis (above) and the main planar system (below). The experimental data is shown for T-phase $Al_{62}Cu_{20}Co_{15}Si_3$. Left column: PIXE with same symbols for the elements as in Fig. 1 and TM–RBS with crosses. Right column: RBS with circles for Al and triangles for TM. The lines represent the calculated profiles for the MII model with a phason disorder of 0.27 and an angular spread of $\pm 0.1^\circ$. The PIXE profiles for Co and Cu in the axial case (above) have been adjusted by an offset of 0.15 and 0.19 respectively [15].